

4.4.4 RESIDUAL BULK IMAGE

Reference 4.4.4-1 - IOM CLK-387-178-6.3.1 / ISS DFM 387-CLK-96-606, " Residual Bulk Image Effect Final Report", C. Kahn , dated July 9, 1996

Reference 4.4.4-2 - IOM , " More RBI Tests", Tom Elliot, October 17, 1995

Reference 4.4.4-3 - IOM , " A Model for Residual Bulk Images, Update #2", Gary Yagi, September 5, 1997

Reference 4.4.4-4 - IOM 388-PAG-CCA97-3, "WAC FM Calibration Results: Dark Current", Charlie Avis, March 6, 1997 (see Section 5.1.5.2)

4.4.4.1 BACKGROUND

As reported in Reference 4.4.4-1 (modified for continuity and exclusion of attachments)

The Cassini ISS charge coupled devices (CCDs) exhibit a phenomenon called the Residual Bulk Image (RBI) effect. RBI is the ability of the CCD to trap electrons in the bulk material (due to bulk state defects) and then release them slowly into the pixel wells. This effect is highly temperature dependent. At warm ($> -40^{\circ}\text{C}$) temperatures, RBI is rarely seen because the time constant of the electrons from the bulk material into the wells is very short. At very cold temperatures ($< -110^{\circ}\text{C}$), the effect is not seen because the time constant of the electrons is very long - essentially, the electrons become "frozen" in the bulk material. RBI is best seen between temperatures of -50°C and -100°C when a saturated image of a target is taken followed by a dark frame. The dark frame will show a distinct shadow of the target. Since the Cassini ISS CCDs are controlled to a temperature of -90°C , the effect is present. A memo written by T. Elliot (Reference 4.4.4-2) describes test conditions for characterizing RBI at -90°C . Figure 4.4.4-1 (Image 1 of Reference 4.4.4-2) is a dark frame which clearly shows RBI.

In order to control the RBI effect in the system, a technique of light flood and erase is used. This technique uses IR LEDs, centered at 900nm, to saturate the CCD bulk material prior to every image with an erase cycle to remove any charge from the pixel wells prior to the start of integration. The light flood and erase times are constant for every image. This approach provides a stable platform for each image so that the RBI effect will not be present.

A series of tests was run with the NAC engineering model to determine the correct light flood time (the erase time is set by the pixel timing control in the ISS electronics) since the amount of saturation is critical in eliminating the shadow image but also introduces noise. A bar target was imaged to at least 10x full well and then dark images were taken. Varying light flood durations were programmed from 0 msec to 500 msec in 50 msec steps. The images were scanned visually and a frequency analysis was used to look for the shadow image of the bars in the dark frame. From this data, a light flood duration of 200 msec was chosen. This was the shortest amount of time at which no evidence of RBI could be seen. It should be noted that this duration is programmable and, if necessary, can be changed in flight.

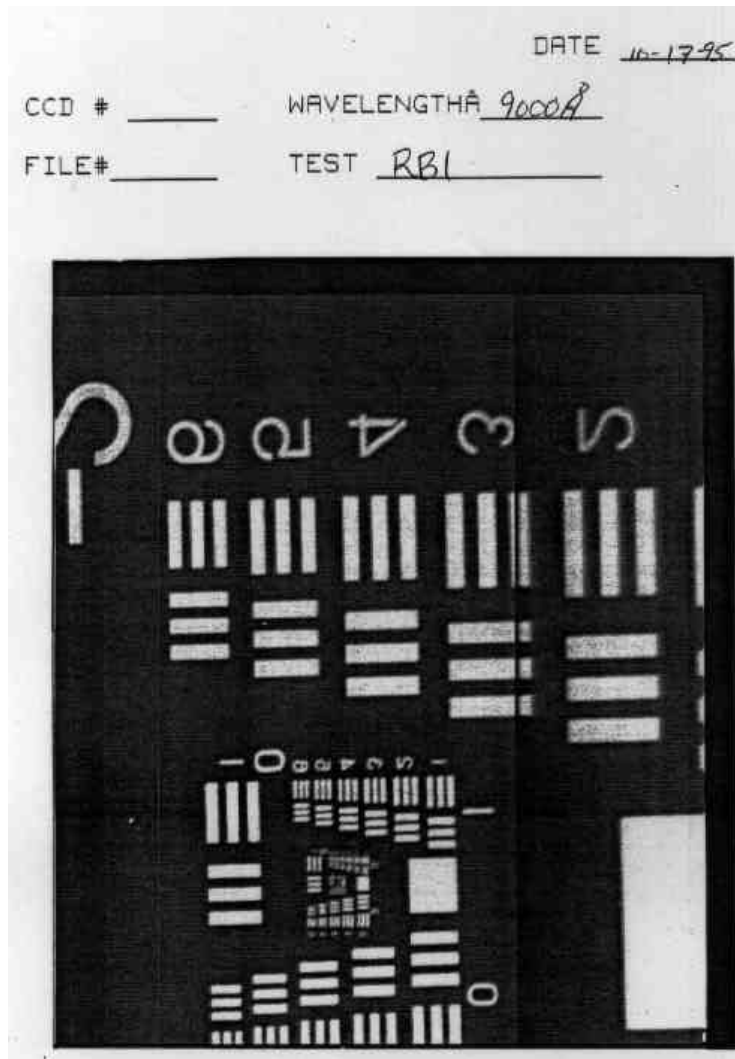


Figure 4.4.4-1 - Dark Frame Exhibiting RBI

Even though the major impact of RBI (shadow images) is eliminated, the use of the above described technique is not perfect at -90°C . The electrons have a finite time constant at this temperature. Two questions were raised: (1) is the quantum efficiency of the system using light flood stable and (2), since the amount of additional signal in an image from RBI is dependent on the integration time, can this effect be modeled?

A test to determine the stability of the quantum efficiency (QE) was devised with the support of R. West of the ISS science team. Two sets of ten images was taken for each summation/gain combination in the instrument. The first set was acquired at low signal levels (.2 full well), the second set at high signal levels (.8 full well). The exposure time was constant within each set. Variation in DN level (which, in a perfect test, is a system level way of looking at QE) were plotted. [NOTE: It is known now that the light source used for this test was experiencing some instability due to power supply problems. This effect has been estimated to contribute approximately 0.5% error to the following data]. The tabulated data and plots are given in Attachment 2 of Reference

4.4.4-1 (not included here). For any summation/gain combination, the variation from frame to frame is less than 2% and in most cases is less than 1%. Three areas in each frame were plotted - top, middle, and bottom. No significant variation is seen for a particular area of the chip and the variability of the QE is not systematic, i.e. there is no directional trend in the data.

To answer the second question, an extensive program was undertaken to attempt to model the RBI effect. Test data was taken at all summation/gain combinations and various exposure times (0 msec to > 5 minutes) [NOTE: From T. Elliot's data it appeared that the bulk state time constant was slightly over three minutes]. The final result, however, is that a complete model was not able to be developed. Even though when plotted, the data appeared to have a structure that could be determined, repeated attempts to fit the data to a combination linear/exponential model and determine the coefficients failed. A representative model and plots showing the approach used and indeterminate results is given in Attachment 3 of Reference 4.4.4-1 (not included here). *Note: Although this initial effort to model RBI was unsuccessful, a subsequent attempt to model RBI was made and is reported below in Section 4.4.4.2.*

4.4.4.2 RESIDUAL BULK IMAGES MODEL

As reported in Reference 4.4.4-3 (modified for continuity within this report & addition of Mode 5 note)

Presented below are the results from an effort to model the effects of the residual bulk image (RBI) arising from the light-flood/erase steps preceding the exposure of an image via the Cassini ISS camera. Included below are (1) a model of RBI, (2) a timing model for the camera, and (3) an analysis of the location of the line break in 1x1 summation mode images. Unless specifically indicated, all results are based on data obtained from the WAC at telemetry modes 1 and 6 (see Reference 4.4.4-1 and Reference 4.4.4-4).

The motivation for the above analysis was to account for the RBI charge deposited in a given pixel in exposure predictions related to the Cassini Planning Tool. The results may also prove useful in the radiometric calibration of the flight data.

The RBI model:

$$y = a(1 - e^{-bt}) \quad (\text{Equation 4.4.4.2-1})$$

where

t is the time from light-flood/erase to readout of a given pixel,
y is the number of RBI electrons deposited in the pixel in t seconds,

and a and b are constants to be determined by fitting the model to image data (unshuttered) acquired in the light-flood/erase mode.

Note that at time t=0, y=0, and at time t=infinity, y=a.

The data used to determine constants a and b are from Reference 4.4.4-4 (see table of exposures vs frame-wide mean DN at gain 3). Since the mean DN for a zero exposure frame taken at telemetry mode 6 is approximately 6, 6.1 was added to all the DN values to add back the data subtracted in

the bias correction step. The DN values were then converted to electrons by multiplying by a system gain constant of 11.42 electrons/dn.

A mean readout time was added to each exposure time to obtain the time t . If the entire image were simultaneously read out of the CCD at the mean readout time, the resulting (constant) DN would equal the mean DN derived by performing the frame-wide averaging. Note that the mean readout time is less than half the readout time since the first 495 lines are read out at a much faster rate than the remainder of the image (see discussion of camera timing model below).

The IDL routine CURVEFIT was used to fit the above data to Equation 4.4.4.2-1. (By a remarkable coincidence, the example given in CURVEFIT uses the same model.) The results from that fit are (see Figure 4.4.4-2):

$$a = 339.741 e^- \quad \text{and} \quad b = 0.0102778 \text{ sec}^{-1}$$

The RMS error was $1.31406 e^-$. The model (Equation 4.4.4.2-1) appears to break down at high exposures.

After reviewing the results above, Bob West pointed out that the rate at which electrons are deposited by the RBI is a function of the size of the trap in the bulk state. He suggested that the exponential term above be replaced by three similar terms, representing three different trap sizes (in theory there is a continuous range of trap sizes). The revised model is as follows:

$$y = a_1(1 - e^{-b_1 t}) + a_2(1 - e^{-b_2 t}) + a_3(1 - e^{-b_3 t}) \quad \text{(Equation 4.4.4.2-2)}$$

Fitting this model to the data yields the following coefficients for the WAC (see Figure 4.4.4-3):

$$\begin{array}{ll} a_1 = 183.404 & b_1 = 0.00267018 \\ a_2 = 182.288 & b_2 = 0.0143802 \\ a_3 = 62.1478 & b_3 = 0.0878187 \end{array}$$

The RMS error was $0.08776 e^-$.

Fitting the model to corresponding data from the NAC yields the following coefficients (see Figure 4.4.4-4):

$$\begin{array}{ll} a_1 = 176.321 & b_1 = 0.00196861 \\ a_2 = 223.611 & b_2 = 0.00953828 \\ a_3 = 70.2694 & b_3 = 0.109124 \end{array}$$

The RMS error was 0.218677.

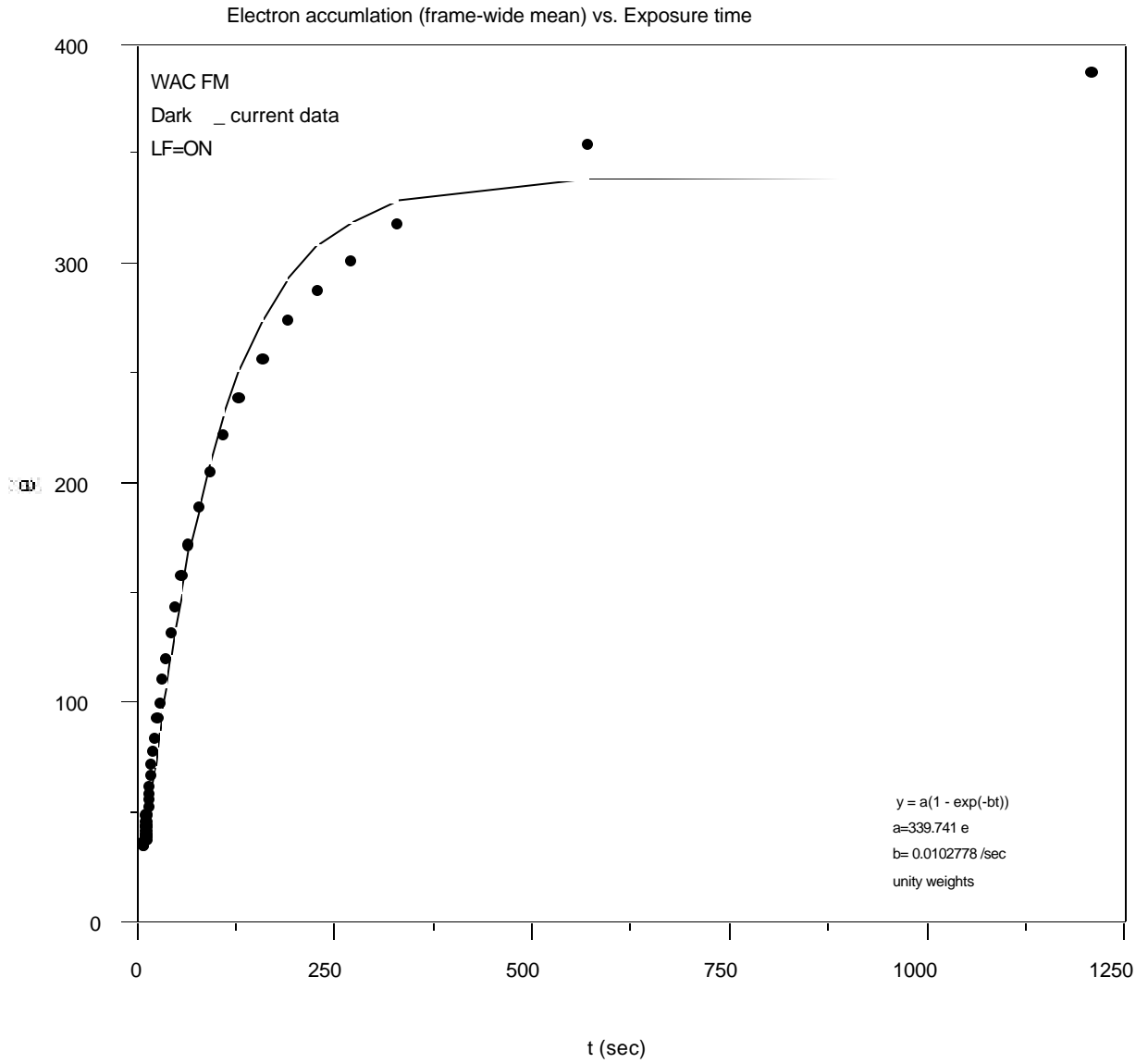


Figure 4.4.4-2

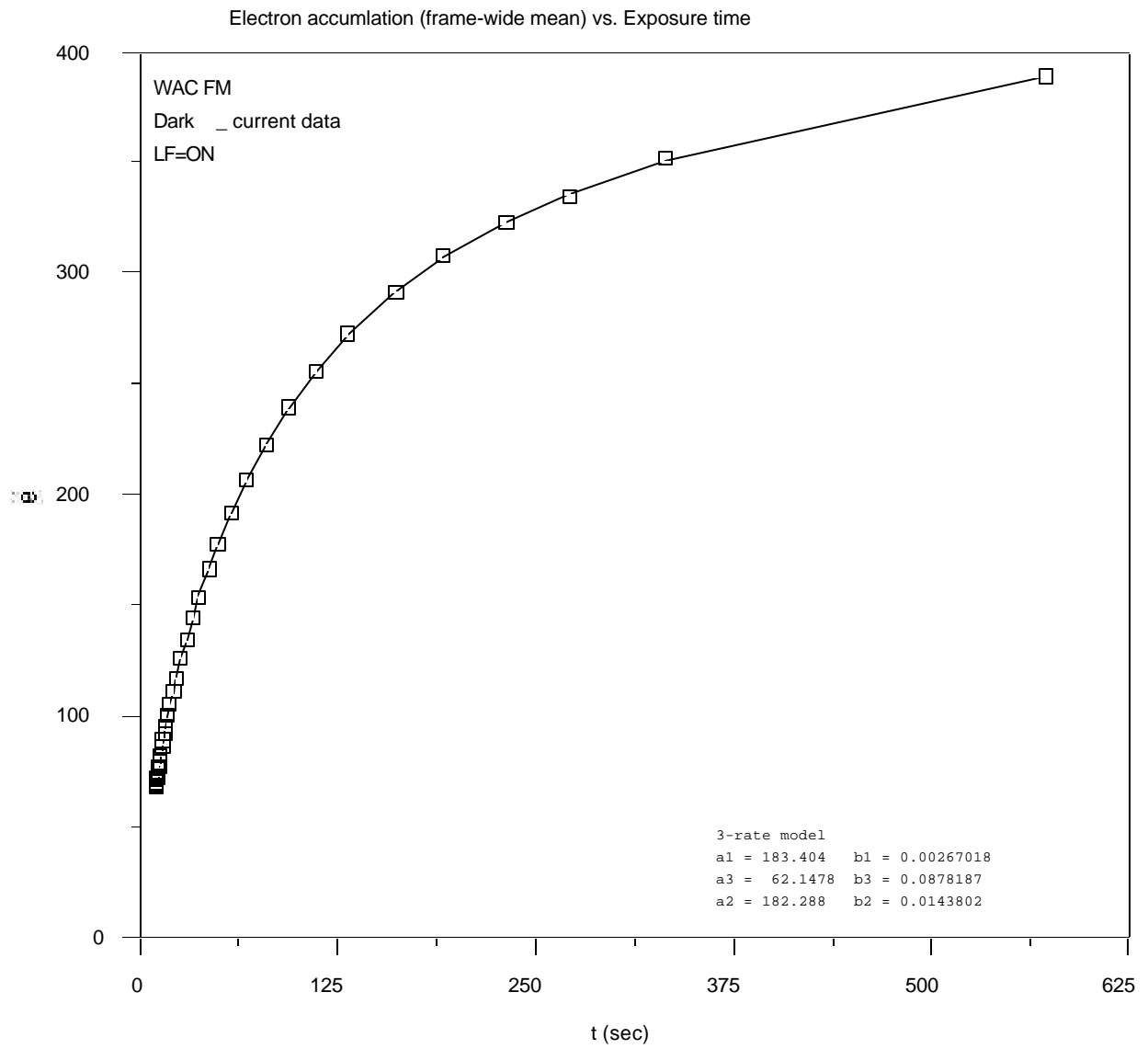


Figure 4.4.4-3

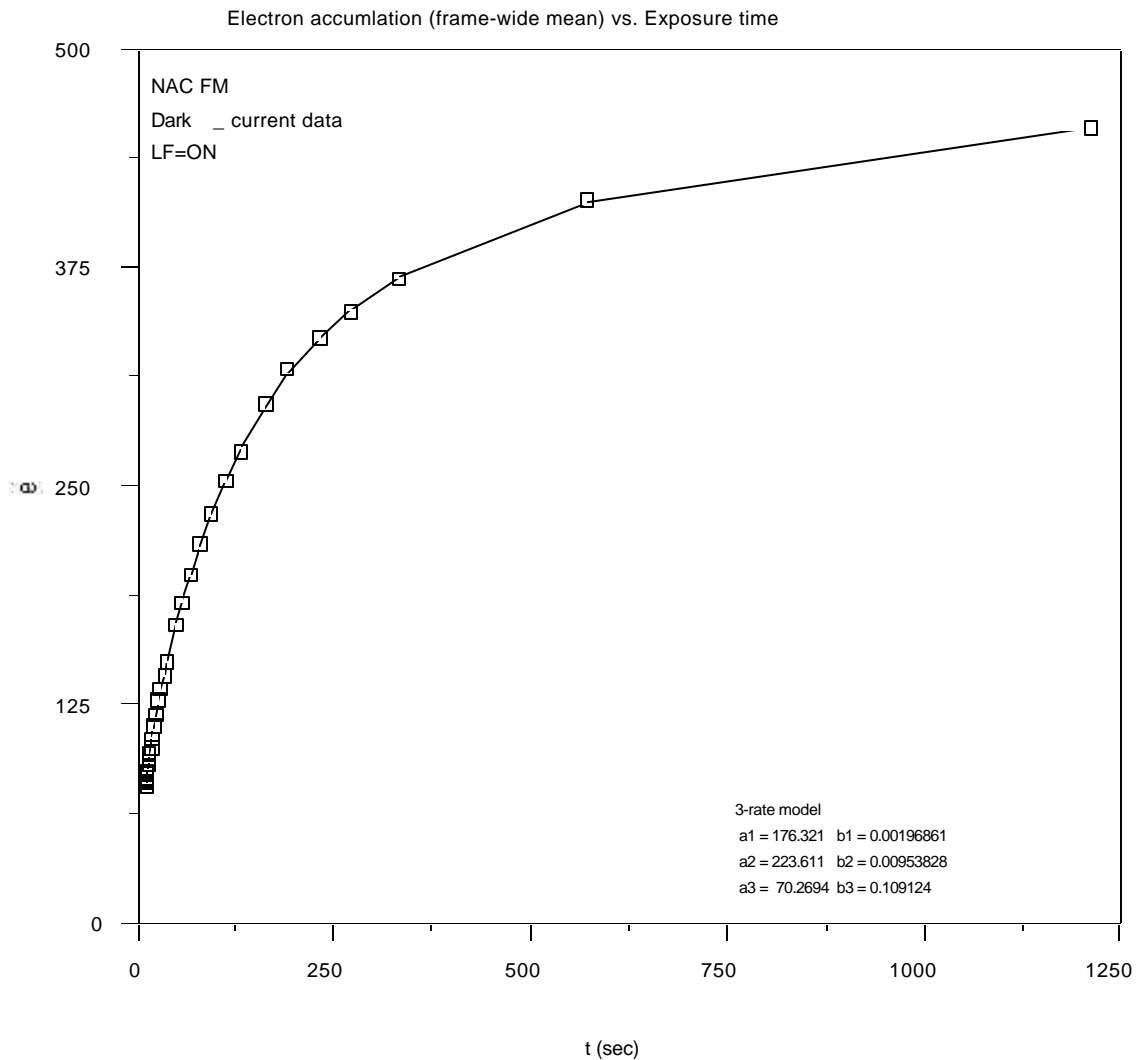


Figure 4.4.4-4

Charles Avis used the above RBI model to predict the DN value at each image line of a zero-exposure frame taken at the lowest gain state and at the highest telemetry mode. Figure 4.4.4-5 and Figure 4.4.4-6 are a comparison between the predicted and actual DN values for the WAC and NAC, respectively. A bias correction has been applied to the actual data.

The RBI model does not account for the spatial dependence in RBI build-up. This spatial dependence is due to non-uniform LED illumination during light flooding. This results in a shading pattern in the image, with the center of the image approximately 10% brighter than the corners (for this example).

Line Profile for Exp=0 -- Model vs. True

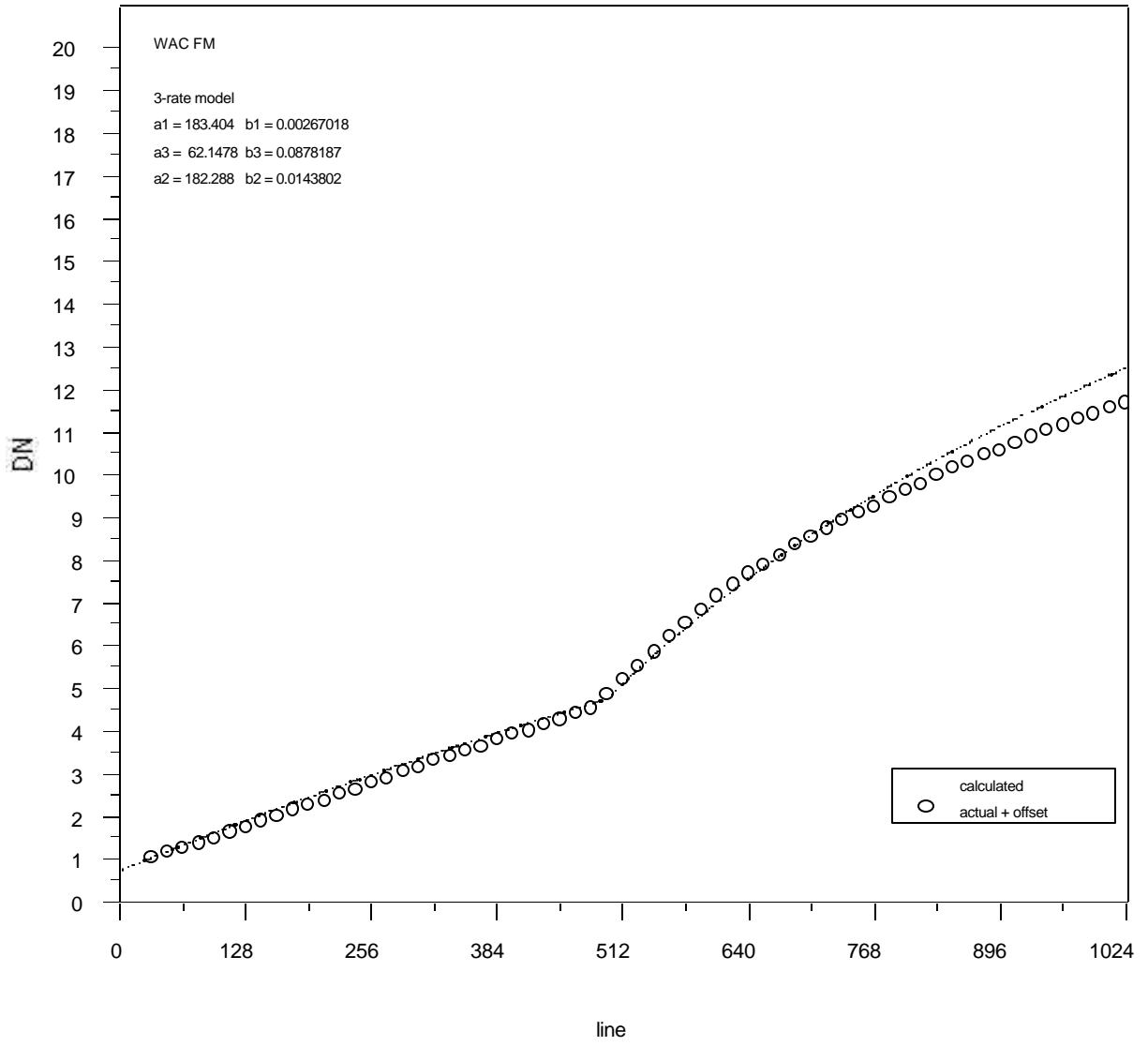
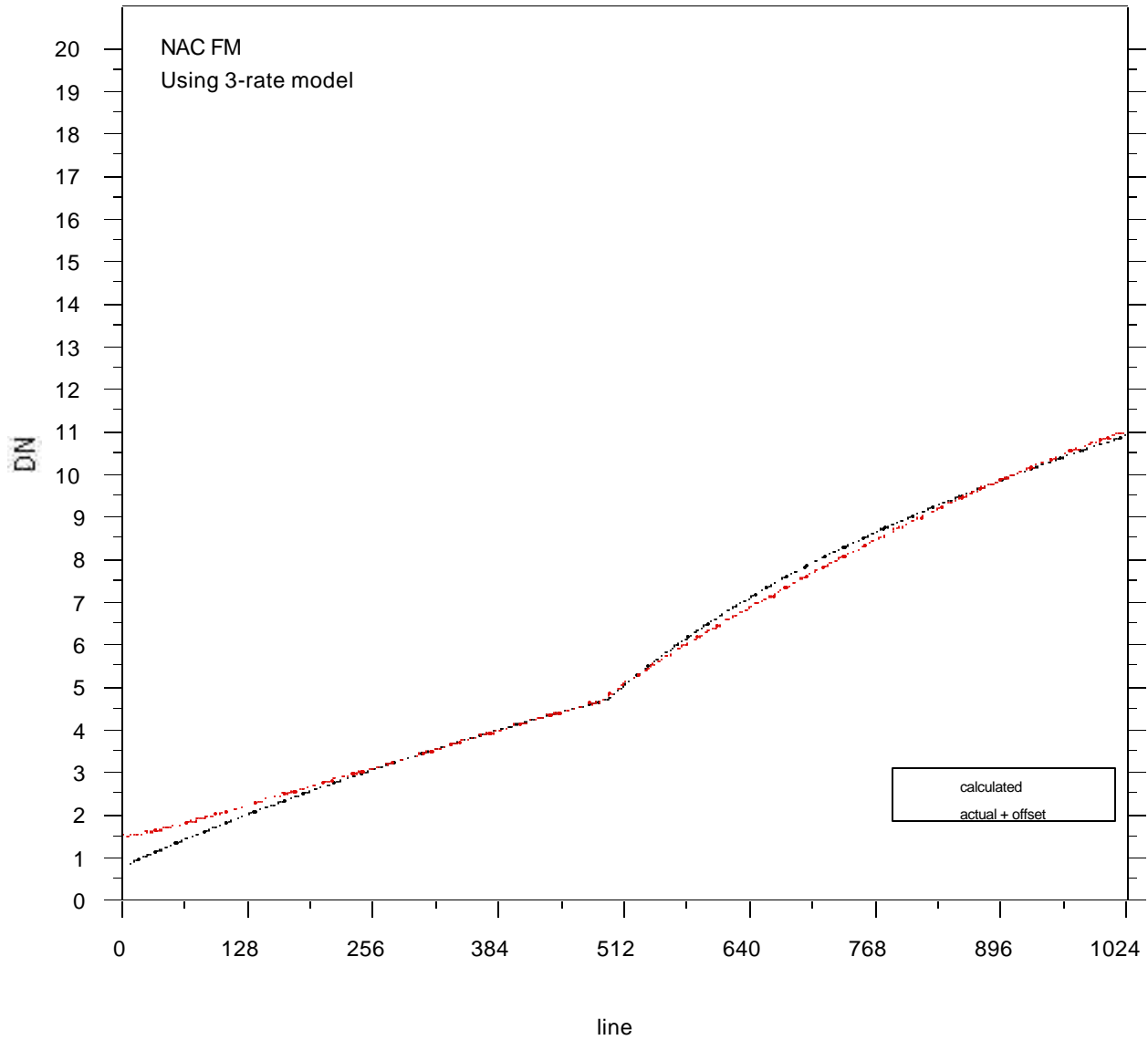


Figure 4.4.4-5

Line Profile for Exp=0 -- Model vs. True

**Figure 4.4.4-6**

(Note for Figure 4.4.4-6 : The "actual +offset" line profile (red) can be identified as follows : the top line from ~ lines 0 to 512, the bottom line from ~ lines 513 to 832, and the top line from ~ lines 833 to 1024.)

The Camera Timing Model:

Since RBI build-up is a function of time (Equation 4.4.4.2-1), it is necessary to compute the elapsed time from the light-flood/erase step to data read-out. Mike Girard has developed a timing model which allows us to compute this time as a function of image line number.

It has been empirically determined that the ISS camera can read data out of the CCD at the following rates (in lines/sec):

Mode	r ₁ (none)	r ₁ (compression)	r ₁ (conversion)	r ₁ (both)
1x1	68.9655	74.62687	79.3651	79.3651
2x2	87.7193	92.59259	96.15385	96.15385
4x4	156.25			

The data is read from the CCD into a 344,064 pixel buffer (16-bit pixels). In camera modes where the buffer is large enough to hold the entire image, the time t from light-flood/erase (in seconds) is:

$$t = t_0 + \text{line}/r_1 \quad \text{for line} \leq 4$$

$$t = t_0 + \text{line}/r_1 + 0.247 \quad \text{for line} > 4$$

where

- t_0 is the time from light-flood erase to the first line read.
- r_1 is the CCD readout rate in lines/sec (see table above).
- line is the image line number.

The 0.247 seconds delay is caused by a BIU swap at line 5. We compute t_0 as follows:

$$t_0 = 0.680 \times \left(\frac{1024 - \text{line}}{1024} \right) + \text{exposure time} + .0004 + .0086$$

The first term in the above expression is due to the 680 milliseconds required to erase the CCD following light flooding. For simultaneous exposures, the above equation is valid for both images.

For those camera modes where the image does not fit into memory, a race condition exists between the rate at which the camera fills memory and the much slower rate at which the data is retrieved from this memory for telemetry packetization. When the memory gets filled up, the ISS must transfer data at a slower rate to avoid overwriting data not yet packetized. The line number where the camera switches to this slower rate is needed to compute time t as a function of line number.

Since the number of image pixels will only exceed the memory size of the buffer in 1x1 summation mode, only this mode need be considered. Since the buffer size is 344,064 pixels, it will hold 336 image lines (1024 pixels per image line).

The memory race condition can be modeled as follows:

$$(r_1 - r_2) t = 336$$

where

- r_1 is the CCD readout rate in lines/sec.
- r_2 is the telemetry rate in lines/sec.
- t is the time it takes for memory to fill up.

During time t , $r_2 t$ lines have been transmitted via telemetry. Therefore, the total number of lines that can be read out before memory is filled up is $r_2 t + 336$.

The above model does not account for delays in CCD readout or telemetry transmission. If we account for the 0.247 second delay due to the BIU swap at line 5, the above formula becomes:

$$r_1(t - 0.247) - r_2 t = 336$$

or

$$t = (0.247r_1 + 336)/(r_1 - r_2) \quad (\text{Equation 4.4.4.2-3})$$

The telemetry rate is a function of telemetry mode as follows:

$$r_2 = 3.60494 \times \text{mode} \quad (\text{lines/sec})$$

where mode = 1, 2, 3, 4, 5, or 6. The derivation of these rates is included in the last section of this memo.

By applying these rates to Equation 4.4.4.2-3, we obtain the following values for the line break as a function of telemetry mode:

Mode	r_2 (lines/sec)	t (sec)	line break
1	3.60494	5.37074	355
2	7.20988	5.68425	377
3	10.8148	6.03664	401
4	14.4198	6.43560	429
5	18.0247	6.89103	460
6	21.6296	7.41583	497

The line breaks for telemetry modes 1 and 6 have been empirically determined to be 355 and 496, respectively. This agrees well with our model. An important consequence of this close agreement is that it helps to validate our calculation of rates r_1 and r_2 .

We can now give the equations relating time to image line number for the cases where the image does not fit into memory:

$$\begin{aligned} t &= t_0 + \text{line}/r_1 && \text{for line} \leq 4 \\ t &= t_0 + \text{line}/r_1 + 0.247 && \text{for } 4 < \text{line} < n \\ t &= t_0 + n/r_1 + (\text{line}-n)/r_2 + 0.247 && \text{for line} \geq n \end{aligned}$$

where n is the image line where the line break occurs (from table above).

For simultaneous exposures, the timing for the second image read out is more complex. The first 336 lines are initially read into memory at rate r_1 . The camera then waits until the first image has been completely read out. The remainder of the image is then read out at the slower rate r_2 :

$$\begin{aligned} t &= t_0 + \text{line}/r_1 && \text{for line} \leq 4 \\ t &= t_0 + \text{line}/r_1 + 0.247 && \text{for } 4 < \text{line} \leq 336 \\ t &= t_1 + (\text{line}-336)/r_2 && \text{for line} > 336 \end{aligned}$$

where t_1 is the total time required to read out the first image.

Derivation of the Telemetry Line Rates:

The following is based upon information provided Reference 4.4.4-1 , Attachment #3:

The number of pixels in a packetized image line is 1026 (1024 + 1 extended + 1 overclocked). The number of pixels which will fit into a telemetry packet is 874 or 926, depending on the packet format. At the lowest telemetry mode, the transmission rate is 8 packets per second. At this mode,

$$\begin{aligned} 8 \text{ packets/sec} &= 8 \times 874 \text{ or } 8 \times 926 \text{ pixels/sec} \\ &= 3.406 \text{ or } 3.609 \text{ lines/sec} \end{aligned}$$

One out of every 50 lines occurs at the slower data rate. Therefore the average data rate at the slowest telemetry rate is:

$$(3.406 + 49 \times 3.609)/50 = 3.60494 \text{ lines/sec}$$

The remaining telemetry modes transmit data at a rate 2, 3, 4, 5, and 6 times faster:

Mode	Packets/sec	r2 (lines/sec)
1	8	3.60494
2	16	7.20988
3	24	10.8148
4	32	14.4198
5	40	18.0247
6	48	21.6296

Note : Although Mode 5 @ 40 packets/sec is shown as an option, that telemetry rate is no longer available from the spacecraft.